Temperature and pressure effects on the crystal structure of $Sr_3Ru_2O_7$: Evidence for electronically driven structural responses

H. Shaked,* J. D. Jorgensen, and S. Short
Materials Science Division, Argonne National Laboratory, Argonne, Illinois 60439

O. Chmaissem
Department of Physics, Northern Illinois University, Dekalb, Illinois 60115
and Materials Science Division, Argonne National Laboratory, Argonne, Illinois 60439

S.-I. Ikeda†
Department of Physics, Kyoto University, Kyoto 606-8502, Japan

Y. Maeno
Department of Physics, Kyoto University, Kyoto 606-8502, Japan
and Core Research for Evolutionary Science, Japan Science and Technology Corporation,
Kawaguchi, Saitama 332-0012, Japan
(Received 4 May 2000)

The crystal structure of the ruthenate $Sr_3Ru_2O_7$ as a function of temperature (5–305 K) and pressure (ambient -0.62 GPa) was studied by neutron diffraction. Upon cooling, the lattice parameter c and the rotation angle of the oxygen octahedra φ increase for $305\ \mathrm{K} > T > 50\ \mathrm{K}$, and decrease for $20\ \mathrm{K} > T > 5\ \mathrm{K}$. As pressure is applied at room temperature, the outer apical Ru-O bond expands. This remarkable behavior is discussed in terms of modification of the occupation of energy levels of the Ru^{4+} ion in the crystalline electric field of the oxygen octahedron and a crossover to Fermi-liquid behavior at low temperature. The very anisotropic thermal expansion leads, in sintered powder samples, to a high degree of strain, which is relieved somewhat with each cooling cycle.

INTRODUCTION

The transport and magnetic properties as well as the crystal structure of the ruthenate $Sr_3Ru_2O_7$ have been the subject of several studies in the last few years.[1–11] These studies used samples prepared by one of three methods: (i) Solid-state reaction of powders[1–3,5,8–10] (ii) Flux (F) growth of single crystals,[4,11] and (iii) traveling solvent floating-zone (FZ) growth of single crystals using an image furnace.[6,7] The compound was found to be a metal[1,4,5,7] and a paramagnet at room temperature (RT), with $p_{\mathrm{eff}} \sim 2.5-3.0\mu_B/\mathrm{Ru}$.[1–5,7] Measurements of the electrical resistivity $\rho(T)$ of powders show a notable decrease in ρ with decreasing temperature T beginning at about ~ 20 K.[5] FZ single crystals are highly anisotropic ($\rho_c \gg \rho_{ab}$), and upon decreasing T, ρ_c and ρ_{ab} show remarkable decreases beginning at about 50 and 20 K, respectively, followed by a crossover to Fermi-liquid-like behavior ($\rho = AT^2$) below ~ 10 K.[7] Magnetic susceptibility $\chi(T)$ measurements of powders[1,5] and of FZ single crystals[7] show a peak at ~ 20 K. FZ single crystals, do not show any remnant magnetization down to 2 K.[7] F single crystals did not show the 20 K peak, but were reported to exhibit a transition to ferromagnetism at 104 K, and a remnant magnetization of $1.3\mu_B/\mathrm{Ru}$ at 5 K.[4] No evidence for magnetic ordering at 20 K or 104 K was found in specific-heat measurements[5] or in neutron-diffraction measurements (at 9 and 25 K)[9] of powder samples. A magnetization study of the FZ single crystals under hydrostatic pressure of 1 GPa showed weak ferromagnetism [$\mu(2\ \mathrm{K}) \sim 0.07\mu_B/\mathrm{Ru}$] along the c axis with an ordering temperature of ~ 70 K.[7]

The crystal structure of $Sr_3Ru_2O_7$ (Fig. 1) is a distorted $n=2$ Ruddelsden-Popper (RP) type.[12] The (undistorted) RP structure consists of bilayers (consisting of bioctahedra of oxygen ions), separated by rocksalt layers (consisting of biplanes of SrO). In $Sr_3Ru_2O_7$ the network of octahedra are under compression in the equatorial planes leading to buckling of the shared oxygen [O(3)] apexes which is accommodated by cooperative rotation of the octahedra about the c axis (Fig. 1).[8,10] These rotations lead to a reduction in symmetry from the tetragonal space group[13] $I4/mmm$ (No. 139) of the undistorted RP type to the orthorhombic space-group $Bbcb$ (No. 68) with a pseudotetragonal ($a \sim b$) unit cell, as was recently determined by neutron powder diffraction.[10]

The high anisotropy in the electrical resistivity of $Sr_3Ru_2O_7$ is well understood in view of the layered character of the crystal structure. The RT magnetic moment $p_{\mathrm{eff}} \sim 2.5-3.0\mu_B/\mathrm{Ru}$, measured in powders[1,2,5] and single crystals[4,7] corresponds to $Ru^{4+}(4d^4)$ in a low-spin state in the t_{2g}^4 multiplet of the octahedral crystal field. However, the ubiquitous (except for F crystals) phase-transition-like 20 K peak in $\chi(T)$ with the accompanying changes in $\rho(T)$ are still a mystery. The distinct difference in the magnetic properties of the powders and FZ single crystals (20 K peak) on one hand, and the flux-grown single crystals (ferromagnetism at 104 K) on the other hand, is also not understood. We do, however, make the important observation that pow-

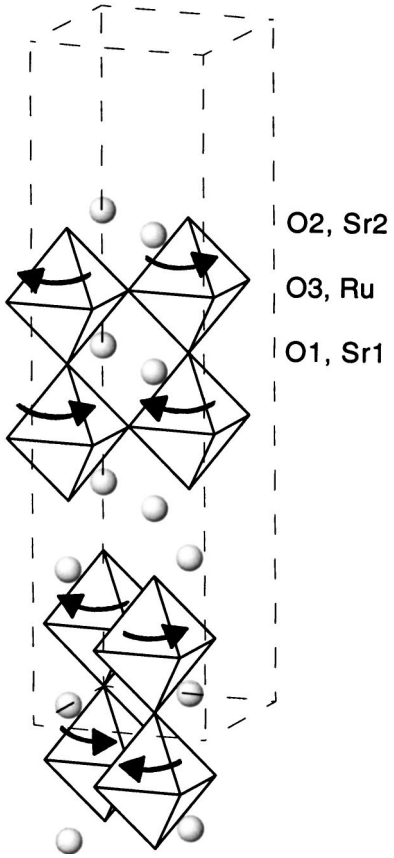

FIG. 1. The bilayered crystal structure of $Sr_3Ru_2O_7$. The large ratio of the ionic radii of Ru (center of octahedron) to Sr (spheres) places the RuO(3) planes under compression. To relieve some of this pressure, the crystal structure responds by rotations (arrows) of the octahedra around the *c* axis.

ders and FZ crystals have the same electrical and magnetic properties, whereas *F* crystals are reported to have different properties.

In the present paper we report the results of a careful neutron-diffraction study of the crystal structure of a powder sample of $Sr_3Ru_2O_7$ as a function of temperature and pressure. The objective of this study, was to obtain detailed temperature and pressure dependences of the crystal structure, in a search of features relating to the remarkable behavior of ρ and χ as a function of temperature and of the magnetization as a function of temperature, pressure, and magnetic field. Neutron diffraction was chosen because of its high sensitivity to subtle changes in the crystal structure, especially those involving the positions of the oxygen atoms in the crystal structure.

EXPERIMENT AND ANALYSIS

A polycrystalline sample of $Sr_3Ru_2O_7$ was prepared by a conventional method of solid-state reaction as described previously.[10] The neutron-diffraction data were collected by the time-of-flight technique using the special environment powder diffractometer[14] (SEPD) at the intense pulsed neutron source (IPNS). The sample mass was 5.0 g. For the temperature-dependent study the sample was mounted in closed-cycle refrigerator. The temperature was varied between 5 and 305 K and the data collected in detector banks at several scattering angles. The data in the backscattering ($2\theta \sim 145°$) detector bank, which gives the highest resolution, were used in the analysis (see below). For the pressure-dependent study the sample was loaded into a helium pressure cell[15] which is mounted on a closed-cycle refrigerator. Pressure was varied between ambient and 0.62 GPa at 300 and 66 K and the data collected only in the 90° detector bank.

The data were analyzed by the Rietveld technique, using the GSAS code.[16] A careful examination of the neutron-diffraction data at all temperatures and pressures did not reveal any change in symmetry. The room temperature (RT) crystal structure as previously determined,[10] belongs to the space-group *Bbcb* (No. 68)[13] with four molecules in a unit cell (Fig. 1). This space group allows for rotation of the oxygen octahedra (Fig. 1) and was used throughout the analyses of the data at all temperatures and pressures. We also included in the analysis a degree of disorder which was introduced as a rotation in the opposite direction (''antiphase,'' see Ref. 10), which refined to a fraction of ~5%.

In the high-resolution data, the 0 0 10 reflection appeared asymmetrically broadened toward the smaller *d* spacing in a way that we were unable to account for with the profile functions in GSAS. This is consistent with a sample strained by stacking faults (which are related to the ''antiphase'' disorder), or by chemical inhomogeneity at the surface of crystallite (due to the high vapor pressure of Ru during synthesis). Fortunately, the asymmetrical broadening did not significantly degrade the structure refinements.

The refined orthorhombic strain, $2(b-a)/(b+a)$, is very small at all temperatures. Thus, it is instructive to consider the pseudotetragonal lattice parameter, $\langle a \rangle = (a+b)/2$, which is shown in Fig. 2 together with the refined lattice parameters *c*, and the resulting unit-cell volume *V*, as a function of temperature. The near-zero orthorhombic strain, $2(b-a)/(b+a)$, is shown as a function of temperature in Fig. 3.

In the pressure experiment, neutron data were collected at the 90° detector bank, which has lower resolution than the backscattering bank and a tetragonal constraint of the lattice parameters, $a=b$, was used in the analysis.

RESULTS

There are four notable features in the temperature dependence of the lattice parameters. (i) Contraction of $\langle a \rangle$ and expansion of *c* as temperature is decreased (Fig. 2). (ii) Below ~20 K, *c* changes from expansion to contraction with decreasing *T* (Fig. 2). (iii) Below 50 K, the small orthorhombic strain decreases and becomes negative (Fig. 3). (iv) In the course of data collection, the sample underwent three cooling cycles (one pressure experiment and two temperature experiments), lasting 2–3 days each. We observed at the end of each cooling cycle that $\langle a \rangle$ decreased slightly while *c* increased slightly (compared to the preceding cycle), notably affecting the $c/\langle a \rangle$ ratio (Fig. 4).

The Ru-O(1) (inner apical) bond length [Fig. 5(a)] and the Ru-O(2) (outer apical) bond length [Fig. 5(b)] increase with decreasing temperature with a change in slope at ~100 K. The Ru-O(3) (equatorial) bond length [Fig. 5(c)] decreases nearly linearly with decreasing temperature. As temperature is decreased, the rotation angle, φ (which accommodates for

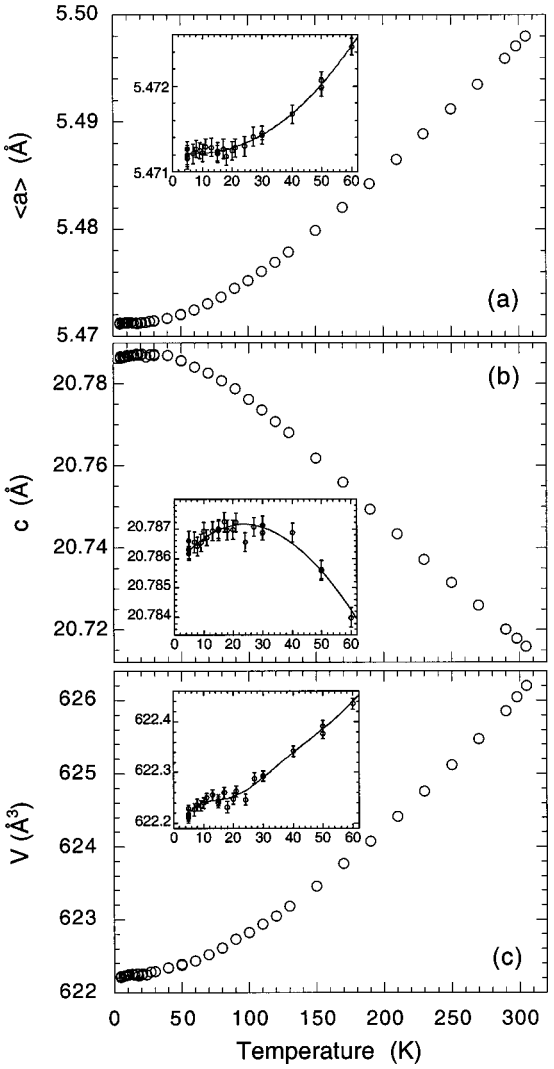

FIG. 2. The refined values of (a) the pseudotetragonal lattice parameter $\langle a\rangle=(a+b)/2$, (b) lattice parameter c, and (c) the resulting unit-cell volume V, as a function of temperature.

the decreasing equatorial [Ru-O(3)] bond length), increases as expected [Fig. 6(a)]. However, below 100 K the slope gradually decreases [Fig. 6(a)], and below 30 K, φ decreases as the temperature is further decreased [Fig. 6(a), inset]. The bilayer thickness increases, and the rocksalt layer thickness

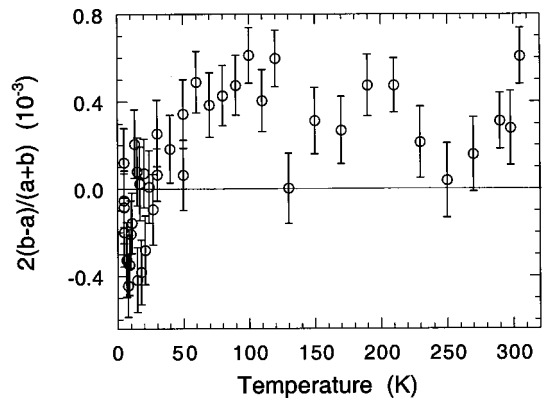

FIG. 3. The refined orthorhombic strain, $2(a-b)/(a+b)$, as a function of temperature.

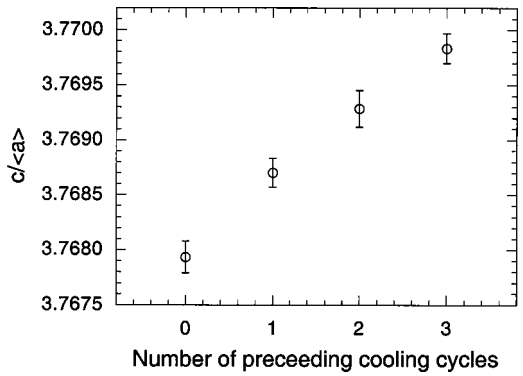

FIG. 4. The ratio $c/\langle a\rangle$ as a function of the number of the preceding cooling cycles.

very slightly decreases as the temperature is decreased [Figs. 6(b) and 6(c)].

The thermal parameters decrease as temperature is decreased (except U_{33}[O(2)] see below), flattening off at low temperature (similar to lattice parameter $\langle a\rangle$). Within the relatively large experimental uncertainty in the value of these

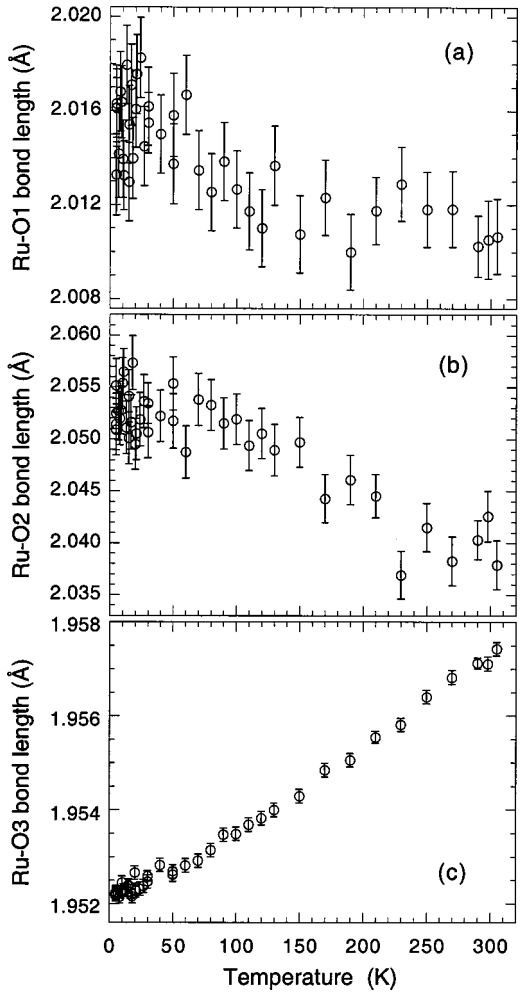

FIG. 5. The refined Ru-O bond lengths as a function of temperature: (a) the inner apical, Ru-O(1); (b) the outer apical, Ru-O(2); and (c) the equatorial, Ru-O(3). The Ru-O(3) bond length is considerably shorter than the unstrained value of 2.02 Å (Ref. 17), and is under compression.

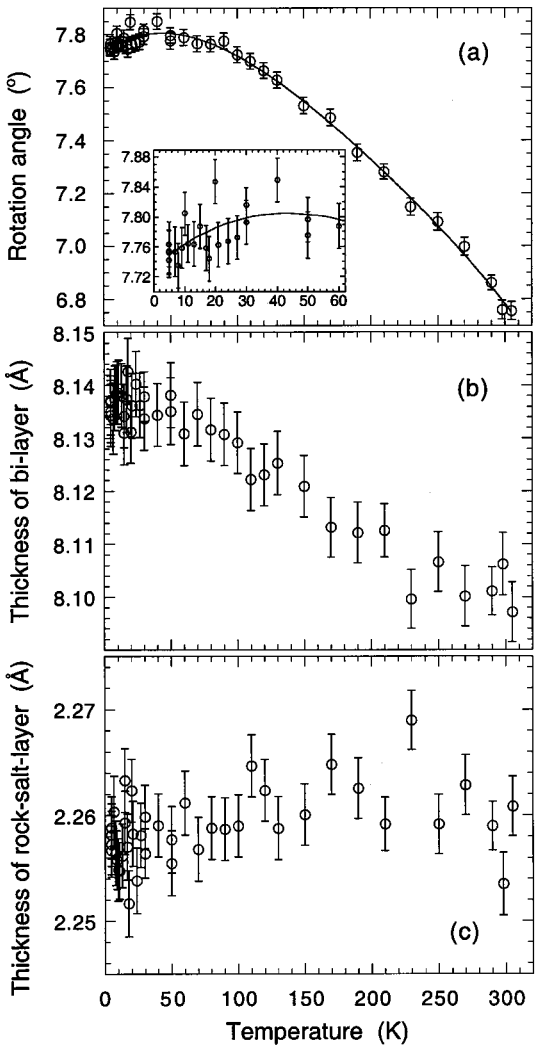

FIG. 6. The refined values of the (a) Rotation angle φ, (b) thickness of the bilayer, and (c) thickness of the rocksalt layer, as a function of temperature.

parameters, no anomalous behavior [like that of $c(T)$ or $\varphi(T)$] is detected at low temperature. The refined value of the thermal parameter for the outer apical oxygen $U_{33}[\mathrm{O}(2)]\sim 0.014(1)\ \text{Å}^2$, is temperature independent, suggesting that some static displacements may be present. However, attempts to model this unusual behavior with disorder in the O(2) site, were unsuccessful.

The hydrostatic pressure on the sample in the pressure cell was varied between ambient and 0.62 GPa. It was found that in this pressure range all crystal parameters changed linearly with pressure [see lattice parameters (Fig. 7), Ru-O(2) bond length and the rotation angle (Fig. 8)]. Compressibilities of crystal parameters were calculated from a linear fit to their refined experimental values versus pressure (Table I).

DISCUSSION

We propose that the anomalous behavior of $c(T)$ and $\varphi(T)$ is driven by changes in the electronic structure associated with the electronic state of the Ru ion. From the observed value of the RT effective magnetic moment, μ_{eff}

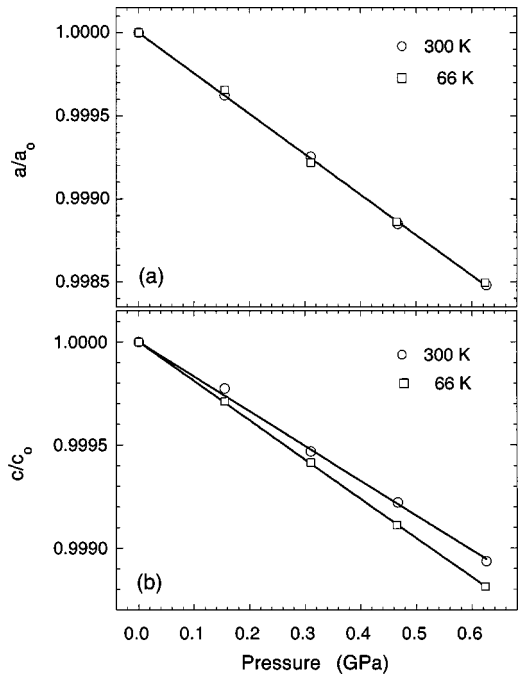

FIG. 7. The refined lattice parameters as a function of pressure at 300 and 66 K, (a) a/a_0 and (b) c/c_0. a_0 and c_0 are the refined values at ambient pressure.

$\sim 2.8\mu_B$ $(S=1)$,[1,3] it is deduced that, at RT, the Ru^{4+} ion $(4d^4)$ occupies the low-spin state, t_{2g}^4, e_g^0. With the symmetry of the elongated ($\sim$3.4%) octahedron in $Sr_3Ru_2O_7$, d_{xz}^2 and d_{yz}^1 (or d_{xz}^1 and d_{yz}^2) have lowest energy with d_{xy}^1 at the next energy level. The separation of d_{xy} from the lowest energy level is proportional to the elongation.

Qualitatively (and naively), it can be argued that as this energy separation increases and becomes comparable to the

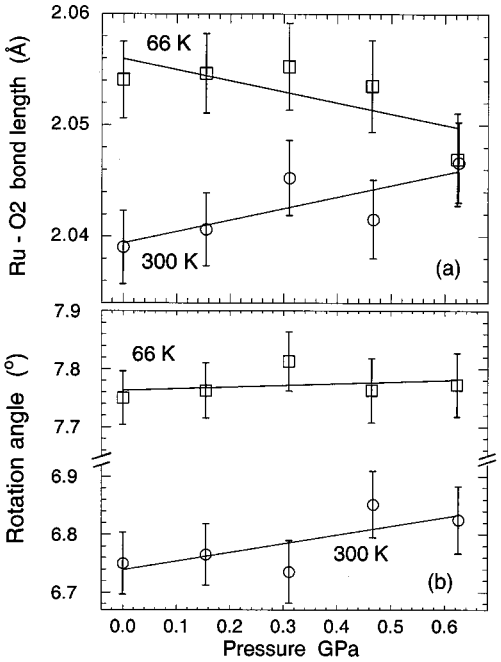

FIG. 8. The refined values of the (a) outer apical bond length Ru-O(2), and (b) rotation angle φ as a function of pressure at 300 and 66 K.

TABLE I. Selected compressibilities κ_L, bulk modulus B, and compression anisotropy of the crystal lattice κ_c/κ_a, obtained from linear fits to the refined parameters of $Sr_3Ru_2O_7$. Compressibility for parameter $L(P)$, κ_L, is defined as $-(dL/dP)/L(0)$ (where P is the pressure). Results for Sr_2RuO_4 (Ref. 18) are presented for comparison.

		$Sr_3Ru_2O_7$		Sr_2RuO_4	
Property	Units	300 K	66 K	300 K	60 K
κ_a	10^{-3} GPa^{-1}	2.44(1)	2.43(3)	2.24(6)	2.12 (2)
κ_c	10^{-3} GPa^{-1}	1.68(2)	1.90(1)	2.56(2)	2.49 (1)
$\kappa_{c/a}$	10^{-3} GPa^{-1}	0.73(5)	0.54(5)	0.32(3)	0.37 (2)
κ_v	10^{-3} GPa^{-1}	6.55(3)	6.76(6)	7.02(4)	6.72 (6)
$\kappa_{\text{Ru-O1}}$	10^{-3} GPa^{-1}	5(2)	1(5)		
$\kappa_{\text{Ru-O2}}$	10^{-3} GPa^{-1}	−5(2)	4(4)	1.9 (7)	2.9(1.4)
$\kappa_{\text{Ru-O3}}$	10^{-3} GPa^{-1}	2.2 (1)	2.4 (1)	2.24(2)	2.12 (2)
B	GPa	153(1)	147(1)	142(1)	149(2)
κ_c/κ_a		0.78(1)	0.69(1)	1.14(3)	1.17 (4)

energy required to pair two electrons in d_{yz} (or d_{xz}), it will lead to $S=0$ (and consequently $\mu_{\text{eff}}\sim 0$). This is indeed observed in Sr_2RuO_4, where, throughout the temperature range 15 K to RT, elongation is 6.8% (Ref. 18) and $\mu_{\text{eff}}\sim 0$ (close to a Pauli paramagnet).[19] In $SrRuO_3$, on the other hand, where distortion of the oxygen octahedron is small,[20] as the temperature is lowered, the magnetic moment prevails and ferromagnetic order sets in at 160 K.[21] In $Sr_3Ru_2O_7$, upon cooling, the elongation increases from 3.4% at RT, where $\mu_{\text{eff}}\sim 2.8\mu_B$/Ru), to 4.2% at 15 K where μ_{eff} is much smaller (magnetization $M<0.25\mu_B$/Ru at 5 K and 5 T).[6] Thus, the modification (mentioned above) in the occupancy of the d orbitals provides an explanation for the enormous reduction in μ_{eff} upon cooling. It is the contraction of the lattice parameter $\langle a\rangle$, which drives this modification in the occupation of the orbitals in the t_{2g} multiplet, in such a way that the octahedra elongate and c expands upon cooling. At about 60 K there is a noticeable slowing in the rate c increases with cooling, and at 20 K, c starts to decrease with cooling. Here the occupancy modification mechanism fails, indicating the emergence of a new mechanism, most likely due to a new electronic state.

The effect of pressure is more complex. When a contracts under pressure, c does not expand (Fig. 7) as one may expect based on the occupancy modification mechanism. However, the c-axis compressibility is considerably smaller than that of Sr_2RuO_4 (Table I) consistent with occupation modification mechanism. The outer apical bond [Ru-O(2)] does expand with pressure increase (Fig. 8) as predicted by this mechanism. Moreover, at 66 K it contracts (Fig. 8) with increasing pressure, signaling the weakening effect of the occupancy modification mechanism at this temperature as observed in $c(T)$.

The increase in the rotation angle, $\varphi(T)$, upon cooling can be explained as an ion size effect. Namely, as the severely compressed Ru-O(3) bond length (Fig. 5) further contracts upon cooling, part of the compression is relieved by an increase in φ. However, as the sample is further cooled below 80 K, the increase in $\varphi(T)$ slows down and changes into a decrease below 30 K. At the same time Ru-O(3) continues to contract almost linearly with cooling. Here, the ion size effect fails and, as for $c(T)$, a different explanation must be provided.

In this temperature region (~20 K), a remarkable peak in $\chi(T)$ and a sharp drop in $\rho(T)$ were observed, upon cooling, in powders[1,5] and FZ crystals.[7] It was suggested that these effects are associated with a crossover to a Fermi-liquid ground state.[7] The anomalous decrease in $c(T)$ and consequently in $V(T)$, upon cooling below 20 K, signals the emergence of a new electron-lattice interaction leading to a large (for low T) thermal expansion coefficient, β. In f-electron compounds, it was shown that Fermi-liquid [heavy fermions (HF)] systems at low temperatures, are indeed characterized by a large β and an unusually large electronic Gruneisen parameter, Γ_e (25 to 150), which is given by[22]

$$\Gamma_e(T)=V_m\beta(T)/\kappa C_e(T) \tag{1}$$

where V_m, β, κ, and C_e are the molar volume, volume thermal-expansion coefficient, volume compressibility, and electronic specific heat, respectively. By substituting $V_m=9.3\times10^{-5}$ m^3/mol Ru (Fig. 2), $\beta(7\text{ K})=1.6\times10^{-6}$ K^{-1} (Table II), $\kappa=6.6\times10^{-12}$ Pa^{-1} (Table I), and $C_e(7\text{ K})=0.6$ J/mol Ru/K (Ref. 5) into Eq. (1), we obtain $\Gamma_e(7\text{ K})=38$. This high value, is indeed characteristic of a Fermi-liquid system. A similar behavior was recently observed in LiV_2O_4, which showed a decrease in $V(T)$ upon cooling, at $T<20$ K, where a crossover from local moment to heavy fermion behavior takes place.[23] A similar calculation in LiV_2O_4 yielded $\Gamma_e(7\text{ K})\sim 25$.

Another potentially important finding of the present work is illustrated in Fig. 4. With each cooling cycle, the sample goes through a ''strain hysterisis loop'' from which it comes

TABLE II. Thermal-expansion coefficients, $\beta_A=(1/A)\ dA/dT$, in units of 10^{-5}/K, estimated from Fig. 1 at RT and at 7 K.

Coefficient	RT	7 K
β_a	2.2 (1)	0.0 (1)
β_c	−1.4 (1)	0.18 (4)
$\beta=\beta_v$	3.2 (5)	0.16 (6)

TABLE III. $c/\langle a\rangle$ values reported for samples of flux grown (F) single crystals, powders, and traveling solvent floating-zone (FZ) single crystals.

Preparation	$c/\langle a\rangle$	Ref.
F crystals	3.716	4
	3.735	11
Powders	3.766	9
	3.768	10
FZ crystals	3.771	7

out less strained and with a slightly shorter $\langle a\rangle$ and a slightly longer c, leading to a larger $c/\langle a\rangle$. This is a result of the opposite signs of the linear compressibilities κ_a and κ_c, and of the strained state of the sample. This explanation is consistent with the following two facts: (i) The FZ crystals, are probably strain free and have the highest $c/\langle a\rangle$ value (Table III). (ii) The powder sample of Ref. 9 was quenched out of the furnace, it is more strained and has a lower $c/\langle a\rangle$ value, than the sample used in the present work which was slowly cooled.[10] As for the cause of the strained state, we can speculate that it could be due to one or any combination of the following effects: (i) Stacking faults, (ii) Grain surface chemical inhomogeneity, (iii) Grain interaction stresses in the sintered powder sample. The very low $c/\langle a\rangle$ value of the flux grown single crystal is more likely due to a slight difference in stoichiometry. Chlorine substitution for oxygen in $Sr_3Ru_2O_7$ would likely require a higher $c/\langle a\rangle$ and is therefore ruled out.

CONCLUSION

Above 50 K, the ruthenate $Sr_3Ru_2O_7$ exhibits expansion of c, and of the bilayer thickness upon cooling, and at RT, the outer apical bond length expands under the application of pressure. This behavior, is explained in terms of a mechanism where a modification in the occupation of the energy levels in t_{2g} occurs as the oxygen octahedra elongate upon cooling. At these temperatures $\langle a\rangle$ decreases upon cooling causing φ to increases due to an ion size effect. Below 20 K, both c and φ decrease upon cooling. This unusual behavior is explained in terms of a crossover to Fermi-liquid behavior as evidenced by previous transport measurements.[7] The sample of the present study exhibited strain, characterized by the value $c/\langle a\rangle$. Each cooling cycle partially relieves this strain, increasing $c/\langle a\rangle$. It is shown that F crystals, powders, and FZ crystals have characteristic $c/\langle a\rangle$ (published) values.

ACKNOWLEDGMENTS

This work was supported by the National Science Foundation, Office of Science and Technology Centers, under Grant No. DMR 91-20000 (H.S. and O.C.) and the U.S. Department of Energy, Office of Science, under Contract No. W-31-109-ENG-38 (J.D.J. and the operation of IPNS), by Ben-Gurion University of the Negev (H.S.), and by the ARPA/ONR at NIU (O.C.).

*Permanent address: Department of Physics, Ben-Gurion University of the Negev, P.O.B. 653, Beer Sheva 84190, Israel.

†Permanent address: Physical Science Division, Electrotechnical Laboratory, Umezono 1-1-4, Tsukuba 305-8568, Japan.

[1] R. J. Cava, H. W. Zandbergen, J. J. Krajewski, W. F. Peck, Jr., B. Batlogg, S. Carter, R. M. Fleming, O. Zhou, and L. W. Rupp, Jr., J. Solid State Chem. **116**, 141 (1995).

[2] M. Itoh, M. Shikano, and T. Shimura, Phys. Rev. B **51**, 16 432 (1995).

[3] S. Ikeda, Y. Maeno, M. Nohara, and T. Fujita, Physica C **263**, 558 (1996).

[4] G. Cao, S. McCall, and J. E. Crow, Phys. Rev. B **55**, 672 (1997).

[5] S. Ikeda, Y. Maeno, and T. Fujita, Phys. Rev. B **57**, 978 (1998).

[6] S. Ikeda and Y. Maeno, Physica B **259–261**, 947 (1999).

[7] S. Ikeda, Y. Maeno, S. Nakatsuji, M. Kosaka, and Y. Uwatoko, Phys. Rev. B **62**, 6089 (2000).

[8] Y. Inoue, M. Hara, Y. Koyama, S. Ikeda, Y. Maeno, and T. Fujita, in *Advances in Superconductivity IX*, edited by S. Nakajima and M. Murakami (Springer-Verlag, Berlin, 1997), p. 281.

[9] Q. Huang, J. W. Lynn, R. W. Erwin, J. Jarupatrakorn, and R. J. Cava, Phys. Rev. B **58**, 8518 (1998).

[10] H. Shaked, J. D. Jorgensen, O. Chmaissem, S. Ikeda, and Y. Maeno, J. Solid State Chem. (to be published 1 November 2000).

[11] Hk. Mueller-Buscbaum and J. Wilkens, Z. Anorg. Allg. Chem. **591**, 161 (1990).

[12] S. N. Ruddlesden and P. Popper, Acta Crystallogr. **11**, 54 (1958).

[13] *International Tables for Crystallography*, *Vol. A*, edited by T. Hahn (Reidel, Dordrecht, 1983).

[14] J. D. Jorgensen, J. Faber, Jr., J. M. Carpenter, R. K. Crawford, J. F. Haumann, R. L. Hitterman, R. Kleb, G. E. Ostrowski, F. J. Rotella, and T. G. Worlton, J. Appl. Crystallogr. **22**, 321 (1989).

[15] J. D. Jorgensen, S. Pei, P. Lightfoot, D. G. Hinks, B. W. Veal, B. Dabrowski, A. P. Paulikas, R. Kleb, and I. D. Brown, Physica C **171**, 93 (1990).

[16] A. C. Larson, and R. B. Von Dreele (unpublished).

[17] R. D. Shannon, Acta Crystallogr., Sect. A: Cryst. Phys., Diffr., Theor. Gen. Crystallogr. **32**, 751 (1976).

[18] O. Chmaissem, J. D. Jorgensen, H. Shaked, S. Ikeda, and Y. Maeno, Phys. Rev. B **57**, 5067 (1998).

[19] J. L. Martinez, C. Prieto, J. Rodriguez-Carvajal, A. de Andres, M. Vallet-Regi, and J. M. Gonzalez-Calbet, J. Magn. Magn. Mater. **140–144**, 179 (1995).

[20] C. W. Jones, P. D. Battle, P. Lightfoot, and W. T. A. Harrison, Acta Crystallogr., Sect. C: Cryst. Struct. Commun. **45**, 365 (1989).

[21] A. Callaghan, C. W. Moeller, and R. Ward, Inorg. Chem. **5**, 1572 (1966).

[22] A. de Visser, J. J. M. Franse, and J. Flouquet, Physica B **161**, 324 (1989).

[23] O. Chmaissem, J. D. Jorgensen, S. Kondo, and D. C. Johnston, Phys. Rev. Lett. **79**, 4866 (1997).